Proceedings of the Institute of Acoustics

MICROPHONE AND LOUDSPEAKER ARRAYS: PRACTICAL LESSONS FROM RADAR, SONAR AND ASTRONOMY

P F Dobbins

BAeSEMA, Marine Division, PO Box 5, Filton, Bristol BS12 7QW

1. INTRODUCTION

Simple arrays of transducers have been employed in sound reproduction systems for many years (eg [1]) in the form of column speakers and gun microphones. These early implementations, although still in common use today, were simple in design and were pre-dated by many years by far more sophisticated examples in the fields of radar, sonar and astronomy.

Recently, however, there has been an upsurge of interest in audio applications of arrays and beamformers, as demonstrated by the number of references found [2-14] in a quick search through some relevant journals for the past few years. This new interest has largely been brought about because advances in computing power and the availability of advanced signal processing chips have made the most sophisticated beamforming techniques a practical proposition for off-the-shelf audio equipment at a sensible price.

In addition to the traditional requirements for controlled directivity in microphones and loudspeakers, the applications considered in the literature include teleconferencing, speech recognition, speaker identification, speech acquisition in an automobile environment, sound capture in reverberant enclosures, large-room recording/conferencing, acoustic surveillance, and hearing aid devices. Such systems rely a great deal on accurate and predictable beamforming and sound source localisation, topics that have been studied extensively in the context of radar, sonar and astronomical applications [15-19].

This paper considers the performance that might be expected in practice from arrays of loudspeakers and microphones based on this experience in the fields of radar, sonar and astronomy.

2. THE CONVENTIONAL BEAMFORMER

Before proceeding to examine the effects of errors and tolerances and other degrading factors, the performance of the most basic array configuration, the Conventional Beamformer (CBF) will be established.

Consider the situation sketched in Figure 1. This shows a number, N, of transducer elements distributed in space along a straight line. It is not necessary, but makes the analysis more straightforward to consider straight line arrays only. This will normally be the geometry adopted

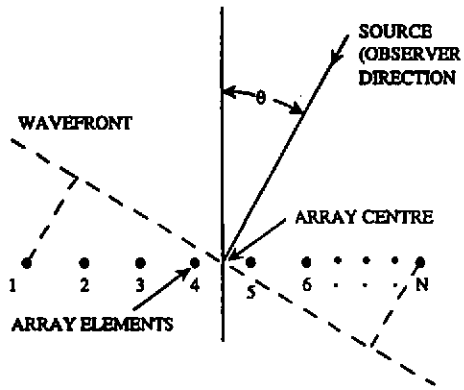

Fig.1 Sketch of N transducer line array geometry.

in audio applications, but it should be remembered that all that follows applies, in principle at least, to any three dimensional distribution of transducers.

Also shown is an acoustic wavefront approaching from a direction θ relative to the normal to the line of the array. This of course makes the assumption that it is an array of receivers (microphones), and most of this description is based on receiving arrays. Again, however, all that follows applies, in principle at least, to arrays of transmitters (loudspeakers).

It should be fairly obvious from Figure 1 that if θ is zero and the wavefront is parallel to the line of the array, then the signals from all the receivers will be in phase, but not in other directions. Thus, if the signals are added together, the total response will be a maximum when θ is zero, and something smaller otherwise. It should also be obvious that phase shifts or time delays could be applied to the signals before adding them to cause them all to be in phase for some other direction of arrival.

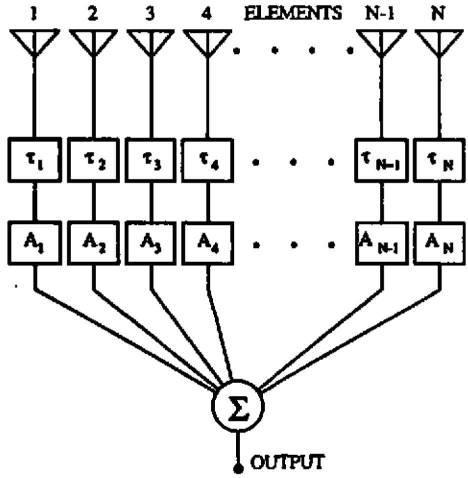

Fig.2 The Conventional Beamformer.

This is the basis of all beamforming, and is all shown schematically in Figure 2. The signals from the N transducer elements are each delayed by a time τ_n, then multiplied by a factor A_n, before they are summed. The A_n, generally known as the shading coefficients or weighting coefficients, control the shape of the directivity pattern, and especially the level of sidelobes in the response, as will be shown below.

Many of the applications discussed in the introduction are based on adaptive beamformers, meaning that the time delays and weighting coefficients can be varied dynamically in response to a changing noise environment or moving source. Only fixed delays and weights are considered here but, once again, all that follows applies, in principle at least, to adaptive systems.

The beamformer as shown in Figure 2 can be represented mathematically by the simple formula

$$S_0(\theta) = \frac{1}{N}\sum_{n=1}^{N} G_n(\theta) A_n \exp\{i(u_n - 2\pi f \tau_n)\} \tag{1}$$

where $S(\theta)$ is the magnitude of the output relative to a single transducer, $G(\theta)$ is the directional response of each individual transducer and f is the frequency. It may be noted here that audio systems are invariably broadband (ie 20Hz - 20kHz), but radar and sonar systems are usually narrowband. Eq(1) describes the response at a single frequency because this allows the simplest representation, but (yet again) all that follows applies in principle to broadband systems.

The term u_n represents the phase of the signal at the nth transducer relative to a reference point at the centre of the array. The formulation for u_n depends on the array geometry and the coordinate system, but for a line of elements, each at some point x_n, and for a directivity represented in polar coordinates, u_n is given very simply by

$$u_n = k\,x_n \sin\theta \tag{2}$$

where k is the acoustic wavenumber, $k = 2\pi f/c$, and c is the speed of sound.

Some example beampatterns are shown in Figure 3 to demonstrate the patterns expected for an ideal array and beamformer, and to identify some parameters of interest. These are all for a 9 element array with the elements spaced half a wavelength apart.

The pattern in Figure 3A is for an unshaded (ie $A_n = 1$) unsteered (ie $\tau_n = 0$) array and shows a distinct main beam at 0° with a series of sidelobes falling away on either side. The beamwidth is normally taken as the width of the main beam where it is 3dB below the peak height. For an unshaded line it is about λ/L radians, where λ is the acoustic wavelength and L is the overall array length, so the beam becomes narrower with increasing frequency and increasing array length. Beamwidths for these example patterns are listed along with the other parameters to be discussed in Table 1.

The maximum height of the sidelobes in this pattern is about -13dB. This is fixed for an unshaded line array and does not change with either frequency or array length.

The beamwidth determines the array's angular resolution, that is the minimum angular separation at which it is possible to separate two sound sources. This is known as the Rayleigh criterion in optics. The ability to reject specific unwanted noise sources outside the main beam depends on the sidelobe level, and the ability to reject isotropic ambient noise is determined by

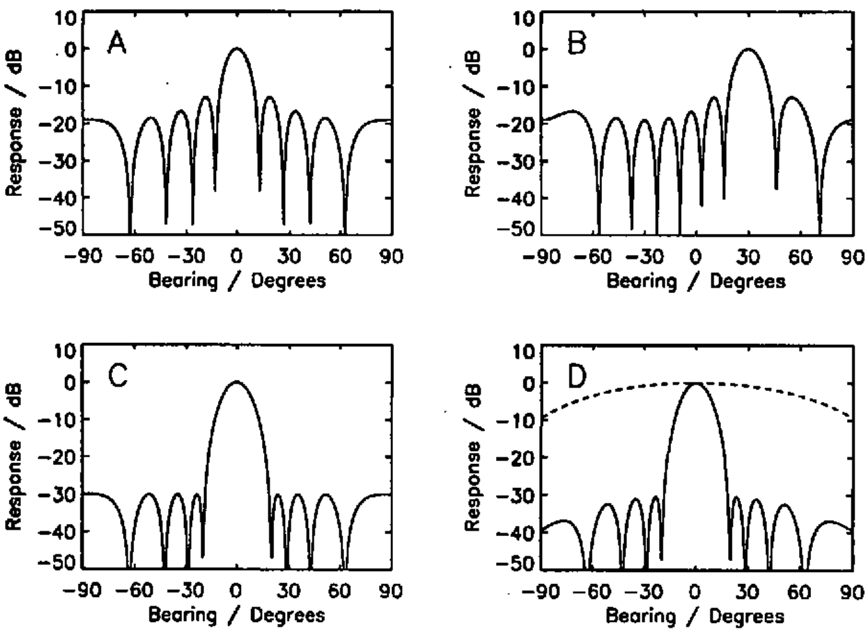

Fig.3 Ideal beampatterns for a 9 element line array with λ/2 spacing demonstrating (A) uniform shading with no steer, (B) uniform shading with 30° steer, (C) Chebychev shading for -30dB sidelobes and (D) the effect of hypercardioid transducer directivity.

the Directivity Index (DI), which depends upon both the beamwidth and the sidelobe level. The DI may be calculated by integrating the beampattern [20], but is reasonably approximated for an unshaded line by $10\log N$. For a loudspeaker array, the DI determines the SPL achieved in the main beam direction for a given power input, while the sidelobes control the amount of 'stray' sound projected in unwanted directions.

Figure 3B shows the effect of steering the array to 30°. The main beam is now pointing at 30°, as expected, but the beamwidth has increased. Analysis of Eqs.(1) and (2) shows that the pattern is actually a function of $\sin\theta$, and if it were plotted against $\sin\theta$, steering would simply result in a sideways translation. When plotted against θ, however, the pattern is stretched as θ increases and when steered to an angle θ, the beamwidth increases approximately as $1/\cos\theta_s$. Although the sidelobes have moved, their maximum level has not changed.

Table 1 Beampattern characteristics for 9 element half wavelength spaced array

Steer Direction	Shading	Transducer Directivity	Beamwidth/ degrees	DI/dB
Broadside	Uniform	Omni	11.33	9.54
30°	Uniform	Omni	13.12	9.54
Broadside	Chebychev	Omni	14.52	8.81
Broadside	Chebychev	Hypercardioid	14.41	14.67

Figure 3C demonstrates how the sidelobes can be controlled by the shading coefficients A_n. The beamwidth increases as the sidelobes are suppressed, and it may be shown [21] that the best compromise between sidelobe level and beamwidth is obtained when the sidelobes are at a uniform level, generally referred to as Chebychev shading. Formulae for generating the coefficients for simple geometries are available [21], and the set used to produce Figure 3C is listed in Table 2. More sophisticated methods [22] allow almost arbitrary shaping of beampatterns, including steering nulls in specific directions, and as suggested in the introduction, this process can be carried out dynamically in adaptive systems [23].

Finally, the previous patterns assumed the individual array elements to be omnidirectional, but Figure 3D shows the effect of transducer directivity. A hypercardioid pattern, shown by the dashed line, has been applied to each receiver. As might be guessed, when the directivity, G_n in Eq.(1), is the same for all elements, the overall pattern is simply the product (or sum in dB) of the array and element beampatterns. Furthermore, the DI's of the two patterns are also added.

3. REAL WORLD BEAMPATTERNS

Having established the behaviour expected from an ideal beamformer, an example of the measured beampatterns of an actual sonar array may prove interesting.

The dashed line in Figure 4 shows the predicted pattern for a plane array, about 4λ diameter, over a full 360° circle, and the solid line shows a measurement with the array mounted on the end of a small cylindrical body.

Table 2 Chebychev coefficients for 9 element λ/2 spaced array, -30dB sidelobes

n	1	2	3	4	5	6	7	8	9
A_n	0.2527	0.4590	0.7194	0.9229	1.0000	0.9229	0.7194	0.4590	0.2527

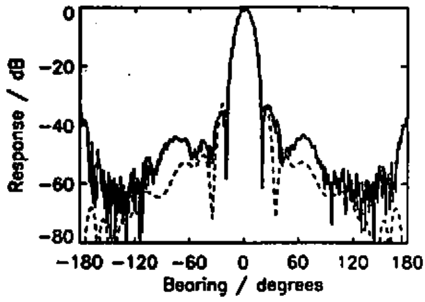

Fig.4 *Predicted (dashed line) and measured (solid line) beampatterns for a planar sonar array.*

Various discrepancies are immediately apparent, but the three most obvious are that the measured sidelobe levels are generally about 10dB higher than predicted, there is a large peak in the backward direction (±180°), and the deep nulls in the predicted pattern are not found in the measurement. The next section will examine the causes of some of these errors.

4. SOURCES OF ERROR

The discussion in Section 2 dealt with ideal arrays. It is obvious however that there are many potential sources of error, both electrical and mechanical.

The main causes of discrepancy between the predicted performance of an array and what is achieved in practice are phase and amplitude variations in the responses of the transducers and various other components of the system. This will be discussed in detail in Section 4.1 below. Two other areas that must be considered are various physical phenomena and environmental effects. There is not space in the present to paper to examine these in depth, but their effects may be summarised:

Physical phenomena such as diffraction and mutual coupling between the transducers also contribute. Such phenomena, however, are complex and difficult to generalise. Their main effect is to modify the responses of the transducers, and as such can be included with system errors and tolerances, but two specific effects should be borne in mind:

- Mutual coupling changes the radiation impedance seen by transducers, which in turn changes the electrical impedance at their terminals. In loudspeaker arrays this may result excessive cone displacement or in lowering the input impedance to a level that results in destructive current flow.

- Diffraction potentially leads to increased responses in unwanted directions, as at ±180° in Figure 4, but it can also distort the individual transducer directivity patterns. In particular, the response of transducers near the edge of a baffle can become asymmetrical. This introduces amplitude errors that are different for different transducers and also change with direction and often results in high sidelobes in the ±90° direction.

Environmental effects may not be significant indoors, but in the open air wind currents and turbulence may distort wavefronts dramatically. The resulting degraded beampatterns are similar to those due to random errors, but fluctuate with time. Such fluctuations are what cause stars to twinkle or objects to waver when seen through a heat haze, and they motivate astronomers to move their imaging systems into space or to employ complex correction techniques [18]. In audio systems they might cause a distant sound source to vary in level or its apparent position to wander.

4.1 System Errors and Tolerances

Transducers are probably the major culprits. Specified accuracies of say 0.1dB in amplitude and 1° in phase might be expected of laboratory microphones, but 1dB and 10° is probably optimistic for production items. With loudspeakers, when the enclosure is considered, the tolerances are probably even worse, say 3dB and 30° for the flatter parts of their response. Near resonances both phase and amplitude vary rapidly with frequency so minor variations in resonant frequency can cause large disparities in response.

These suggested tolerances are mainly intuitive. Except for laboratory instruments, manufacturers' specifications rarely include information about phase responses or tolerances and stability. There do, however, exist some published data concerning the accuracy of microphones of various constructions (eg [24-26]), and the author has conducted limited experiments to check the phase and amplitude matching of two batches of microphones [27]. In these tests the overall rms amplitude errors were 1.5dB for low cost miniature electret microphones (Aoi ECM-1028) and 1.0dB for medium cost dynamic stage microphones (Shure 588SA). The overall rms phase errors were 10° for the electrets and 11° for the dynamic units.

Besides electrical considerations, transducer positioning is important. To put this in perspective, in air at 1kHz the wavelength is about 0.34m, 1° in phase represents a distance of about 1mm. It is certainly possible to locate small microphones to accuracies smaller than this, but with large loudspeaker units it is unlikely that the effective position of the acoustic centre is known to such precision.

Analogue electronics can now be produced with almost arbitrary accuracy, but for production equipment tolerances of the same order as those quoted above for microphones are likely. At higher frequencies, if dealing with high electrical impedances, cable capacitance may become significant. As a general rule, all interconnections between transducers and power amplifier outputs or preamplifier inputs should use the same cable and be of equal length.

In digital systems quantization levels and sampling rates must be adequate. Simply delaying signals by the nearest number of samples represents a phase accuracy of ±90° at the Nyquist rate unless some sort of interpolation is applied. With suitable word lengths and techniques such as FIR all-pass-filters for implementing time delays [28] the errors can be made arbitrarily small

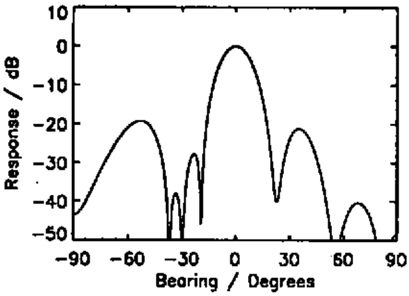

Fig.5 Beampattern of 10 element shaded array with 30° phase and 20% amplitude rms variation.

although, as with analogue electronics, this increases system complexity and cost. Nevertheless, in digital systems the errors are deterministic (although they can be treated as random) so can be evaluated precisely at the design stage [29].

4.2 Evaluation of Error Effects

When all the error sources listed above are taken into account, it may be assumed that they can be resolved into an equivalent overall amplitude and phase variation. Furthermore, because of the many contributing error sources, it may also be assumed that the Central Limit Theorem applies and the overall amplitude and phase variations are zero mean normally distributed random variables, completely described by their standard deviations or rms values. Figure 5 illustrates the deleterious effect of such random errors. This shows the beampattern of the same array as in Figure 3C, but errors have been included and Eq.(1) rewritten

$$S(\theta) = \frac{1}{N}\sum_{n=1}^{N} G_n(\theta)(A_n + \Delta_n)\exp\{i(u_n - 2\pi f\tau_n + \delta_n)\} \tag{3}$$

where Δ_n and δ_n are the amplitude and phase errors associated with the nth element. To realise Figure 5 the Δ_n and δ_n were two independent computer generated Gaussian random number sequences with an rms amplitude variation of 20%, or about 2dB variation in element sensitivity, and an rms phase variation of 30°. It is clearly seen that the sidelobes are distorted and some are raised in level. Also, although not so obvious on visual inspection, there is a slight reduction in main beam sensitivity, the beamwidth is changed, the DI reduced and the beam is no longer pointing towards 0°.

These effects may be quantified, and expressions for the expected beampattern are derived in [30] and [31]. The expected normalised average beampattern is

$$\langle S(\theta)\rangle = \left\{|S_0(\theta)|^2 \exp(-\delta^2) + \left(1 - \exp(-\delta^2) + \Delta^2\right)/L_e\right\}^{1/2} \tag{4}$$

$$L_e = \left(\sum A_n\right)^2 / \sum A_n^{\,2} \tag{5}$$

where S_0 is the error free response, δ is the rms phase error (in radians) and Δ is the rms fractional amplitude error. L_e is the effective length of the array and is equal to N for a uniform array. Even in shaded arrays, however, the value N is a reasonable approximation.

The effect of errors on the performance parameters discussed in Section 2 may be derived from Eq.(4).

The mean main beam peak sensitivity relative to the error free sensitivity is

$$S_{MAX} = \left\{\exp\left(-\delta^2\right) + \left(1 - \exp\left(-\delta^2\right) + \Delta^2\right)/L_e\right\}^{1/2} \tag{6}$$

Phase errors completely swamp the effect of amplitude fluctuations in this expression, so amplitude errors may be neglected, and S_{MAX} is plotted against rms phase error in Figure 6 for $N = 5$, 9 and 15, assuming $L_e \approx N$. The loss in sensitivity is minor (1dB) for an rms phase error of less than 30°. The loss grows rapidly as the phase error increases, but if a sensitivity reduction of about 3dB is allowable, then the graph shows that phase errors up to 50° can be tolerated for any size of array.

The sidelobe level at any given angle is the sum of the value at that angle due to the ideal pattern plus a random quantity due to the phase and amplitude errors. This sets the average minimum sidelobe level achievable in practice. Relative to the main beam, this is given by

$$\left\langle S_{MIN}\right\rangle = \left\{\left(1 - \exp\left(-\delta^2\right) + \Delta^2\right)/L_e\right\}^{1/2} \tag{7}$$

Since the sidelobe level fluctuates about this average level, it is to be expected that peaks of

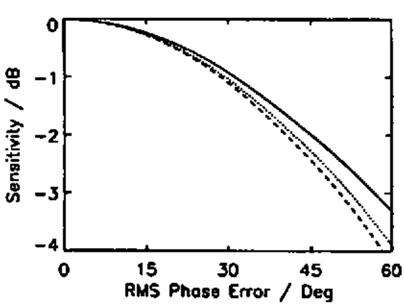

Fig.6 Variation of sensitivity with rms phase error for arrays of 5 (solid line). 9 (dotted) and 15 (dashed) elements.

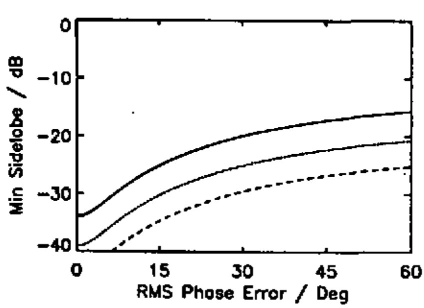

Fig.7 Expected sidelobe level against rms phase error for arrays of 5 (solid line). 9 (dotted) and 15 (dashed) elements.

several times the mean will occur. The maximum likely sidelobe level can be determined from the standard deveiation, again relative to the main beam, given by

$$Var(S)=\left\{\exp\left(-\delta^2\right)+\left(1-\exp\left(-\delta^2\right)+\Delta^2\right)/L_e-1\right\}^{1/2} \tag{8}$$

In practice, peak sidelobe levels are about 6dB above the mean.

Figure 7 shows the minimum average sidelobe level for arrays of 5, 9 and 15 elements, with $\Delta=0.1$, and it is clear that the degraded sidelobe level becomes comparable with the ideal shaded pattern (-30dB) for quite small values of phase variation.

Changes in DI are more difficult to estimate, but it has been calculated [30] for the special case of $\lambda/4$ spacing, and the result gives a reasonable approximation for other spacings. The mean DI is given by

$$DI=10\log\left[\frac{N\exp\left(-\delta^2\right)}{1+\Delta^2}\right] \tag{9}$$

In the limiting case of $\delta=0$ and $\Delta=0$ this reduces to $10\log N$ as expected. DI is plotted against rms phase deviation for arrays of 5, 9 and 15 elements in Figure 8, and it can be seen how the directivity falls with increasing phase errors to a level below that of a smaller array having low error values. It is also clear from Eq.(9) that amplitude errors below about 25% will have negligible effect, so Δ is set to zero in Figure 8.

To demonstrate the plausibility of these results, Figure 9 shows the ideal 9 element shaded beampattern from Figure 3C (dotted line), the perturbed pattern of Figure 5 with 20% rms amplitude and 30° rms phase errors (dashed line) and the average response given by Eq.(4) for the same error values (solid line). It can be seen that the average response gives a reasonable representation of the general sidelobe level, although there are wide deviations from the mean. The peak sidelobe level in the perturbed pattern is about 6dB above the average, as suggested above, and where the sidelobes are low in the no error pattern the average response is about -30dB suggesting that this is just about the lowest achievable sidelobe

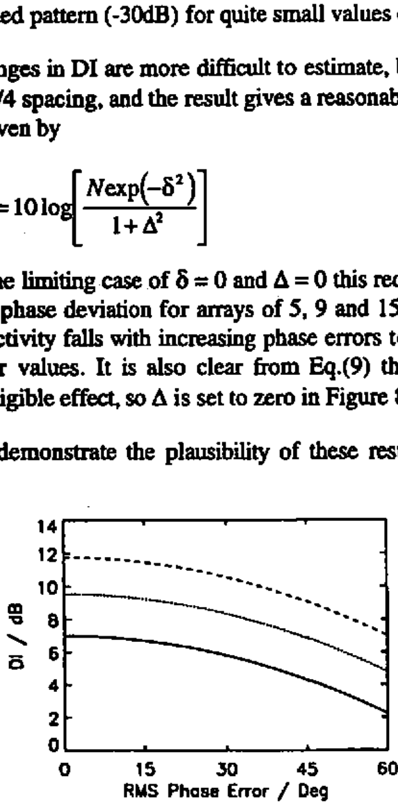

Fig.8 Change in DI against rms phase error for arrays of 5 (solid line), 9 (dotted) and 15 (dashed) elements.

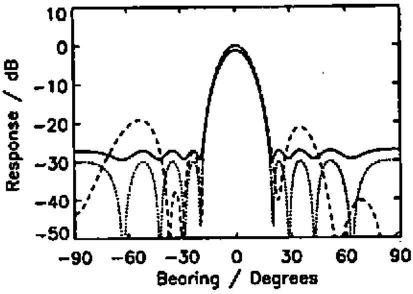

Fig.9 Ideal pattern (dotted line) compared with a single realisation (dashed) and predicted average (solid) for 20% amplitude and 30° phase rms variation.

level. The mean main beam sensitivity in the presence of errors is given by Eq.(6) as -1dB. The average response is seen to be about -1dB, but the perturbed realisation is about 0dB.

5. DISCUSSION AND CONCLUSIONS

The effects of errors on the various array performance parameters discussed in Section 2 must be interpreted with likely applications in mind. In audio work directivity is usually required for one or more of a number of reasons:

i) To improve signal-to-noise ratio (SNR) in the presence of general background noise, or to increase the distance between the microphone and subject.

ii) To suppress the microphone response to a discrete noise source or to nearby loudspeakers, so as to reduce feedback.

iii) To minimise reverberation and echoes by reducing loudspeaker radiation in unwanted directions.

iv) To achieve uniform cover of an audience by controlling the beamwidth of a loudspeaker.

v) To localise a sound source in space or to produce a desired stereo image.

To achieve the first objective requires a high DI, whilst the second and third require a low response away from the main beam. This implies a low sidelobe level or a null steered in a specific direction. The main requirement for objectives (iv) and (v) is that the main beam width, pointing direction and sensitivity are not degraded, and (v) also requires the beam to be symmetrical.

The reduction in DI due to the 30° phase deviation used for the example degraded beampatterns can be seen from Figure 8 to be about 1dB. It is doubtful if this would be noticeable in a practical situation, so it seems reasonable to suppose that, except for the most critical applications, variations in the response of real microphones would not prevent achieving objective (i).

Objectives (ii) and (iii) require low sidelobe levels or a controlled null, and achieving this is more difficult, as can be seen from Figure 7. Arrays of less than nine elements are unlikely to give sidelobes much below about -20dB with the errors and tolerances postulated, so any application needing better than this will need a relatively large array or, alternatively, strictly controlled tolerances. Sidelobes of -30dB are just about attainable with a nine-element array and phase errors in the order of 30°.

Objectives (iv) and (v) need well controlled main beams. Figure 6 shows that if sensitivity variations of about 1-2dB are acceptable, then large errors can be tolerated. However, the effects of errors on pointing accuracy and symmetry are more difficult to estimate. No straightforward analytical formulae are available. However, it may be suggested that the main beam shape will be noticeably disturbed only if the errors are large enough to affect the sidelobes on either side of the main beam. This essentially means that if objectives (ii) and (iii) can be met, then so can (iv) and (v).

The overall conclusion is that the variations in response to be found in real microphones and loudspeakers will not seriously degrade the performance of a directional array in many audio applications. However, where specific performance parameters are significant, system errors and tolerances should be considered at the design stage, and if low sidelobe levels are required then a relatively large array of at least nine elements will be needed.

6. REFERENCES

[1] Beranek, L.L., 'Sound Systems for Large Auditoriums', *J. Acoust. Soc. Am.*, 26, 661 (1954)

[2] Angus, J.A.S. Kershaw, S.M. and Lewis, A., 'An Adaptive Beam-Steering Microphone Array', *Proc. IOA.*, 14(5), 245 (1992)

[3] Forsythe, K., 'Virtual Array Loudspeaker Systems: Design Considerations for "Arrayable" Loudspeaker Systems', *Proc. IOA.*, 14(5), 47 (1992)

[4] Nomura, H., Miyata, H. and Houtgast, T., 'Microphone Arrays for Improving Speech Intelligibility in a Reverberant or Noisy Space', *J. Aud. Eng. Soc.*, 41(10), 771 (1993)

[5] Soede, W. Bilsen, F.A. and Berkhout, A.J., 'Assessment of a Directional Microphone Array for Hearing-Impaired Listeners', *J. Acoust. Soc. Am.*, 94(2 Pt.1), 799 (1993)

[6] Nomura, H., Miyata, H. and Houtgast, T., 'Speech Intelligibility Enhancement by a Linear Loudspeaker Array in a Reverberant Field', *Acustica*, 77(6), 253 (1993)

[7] Khalil, F., Pascal Jullien, J. and Gilloire, A., 'Microphone Array for Sound Pickup in Teleconference Systems', *J. Aud. Eng. Soc.*, 42(9), 692 (1994)

[8] Sydow, C., 'Broadband Beamforming for a Microphone Array', *J. Acoust. Soc. Am.*, 96(2 Pt.1), 845 (1994)

[9] Hoffman, M.W., Trine, T.D., Buckley, K.M. and Van Tasell, D.J., 'Robust Adaptive Microphone Array Processing for Hearing Aids: Realistic Speech Enhancement', *J. Acoust. Soc. Am.*, 94(2 Pt.1), 759 (1993)

[10] Harrell, J.A., 'Constant Beamwidth One-Octave Bandwidth End-Fire Line Array of Loudspeakers', *J. Aud. Eng. Soc.*, 43(7/8), 581 (1995)

[11] Mahieux, Y., Le Tourneur, G. And Saliou, A., 'A Microphone Array for Multimedia Workstations', *J. Aud. Eng. Soc.*, 44(5), 365 (1996)

[12] Van der Wal, M., Start, E.W. and deVries, D., Design of Logarithmically Spaced Constant-Directivity Transducer Arrays', *J. Aud. Eng. Soc.*, 44(6), 497 (1996)

[13] Kates, J.M. and Weiss, M.R., 'A Comparison of Hearing-Aid Array-Processing Techniques', *J. Acoust. Soc. Am.*, 99(5), 3138 (1996)

[14] Liu, C. and Sideman, S., 'Simulation of Fixed Microphone Arrays for Directional Hearing Aids', *J. Acoust. Soc. Am.* 100(2 Pt.1), 848 (1996)

[15] Haykin, S., editor, *Array Processing: Applications to Radar*, Academic, New York, (1980)

[16] Hahn, W., 'Optimum Signal Processing for Passive Sonar Range and Bearing Estimation', *J. Acoust. Soc. Am.* 58, 201 (1975)

[17] Bangs, W. and Schultheis, P., 'Space-Time Processing for Optimal Parameter Estimation', in *Signal Processing*, edited by Griffiths, J., Stocklin, P. and Van Schooneveld, C., Academic, New York (1973)

[18] Muller, R.A. and Buffington, A., 'Real-Time Correction of Atmospherically Degraded Telescope Images through Image Sharpening', *J. Opt. Soc. Am.*, 64(9), 1200 (1974)

[19] Dobbins, P.F., 'Applications of Astronomical Adaptive Optics Techniques to Reducing the Effects of Acoustic Fluctuations', *Traitement du Signal*, 11(4), 301 (1994)

[20] Beranek, L.L, *Acoustics*, Acoust. Soc. Am. (1986)

[21] Dolph, C.L., 'A Current Distribution for Broadside Arrays which Optimizes the Relationship Between Beam Width and Side-Lobe Level', *Proc. IRE Waves & Electrons*, 335-348 (1946)

[22] Dobbins, P.F and Heald, G.J., 'General Shading Technique for Sonar Transducer Arrays', *Proc. IOA.*, 17(3), 117 (1995)

[23] Widrow, B., Mantey, P.E., Griffiths, L.J. and Goode, B.B., 'Adaptive Antenna Systems'. *Proc. IEEE*, 55(12), 2143 (1967)

[24] Sesler, G.M., 'Electret Microphones: A Review', *J. Acoust. Soc. Am.*, 53, 1589 (1973)

[25] Rassmussen, G., 'Measurement Microphones', Inter-Noise 74, Int. Conf. Noise Control Eng., Washington DC, 55-60 (1974)

[26] Hruska, B., Magrab, E.B. and Penzes, W.B., 'Environmental Effects on Microphones of Various Constructions', *J. Acoust. Soc. Am.*, 61(1), 206 (1977)

[27] Dobbins, P.F., 'The Use of Non-Ideal Microphones in Directional Arrays', presented at the 75th Convention of the Audio Engineering Society, Preprint No 2062 (B1), (1984)

[28] Stinchcombe, M.A., 'A Novel Time Domain Beamforming Algorithm Using an Extensible Systolic Convolver Array', *Proc. IOA*., 17(8), 111 (1995)

[29] Butler, D. And Hill, B., 'Beam Steering Distortion due to Interpolation', *Proc. Inst. Acoustics: Advances in Underwater Acoustics*, Underwater Acoustics Group Conference, AUWE Portland, Dec. 1-2 1981, pp 7/1-7/6

[30] Steinberg, B.D., *Principles of Aperture and Array System Design*, John Wiley (1976)

[31] Quazi, A.H., 'Array Beam Response in the Presence of Amplitude and Phase Fluctuations', *J. Acoust. Soc. Am.*, 72(1), 171 (1982)